Published in final edited form as:

Acc Chem Res. 2023 February 21; 56(4): 414–424. doi:10.1021/acs.accounts.2c00648.

Properties of Configurationally Stable Atropoenantiomers in Macrocyclic Natural Products and the Chrysophaentin Family

Carole A. Bewley[*],
Laboratory of Bioorganic Chemistry, 8 Center Drive, National Institute of Diabetes and Digestive and Kidney Diseases, National Institutes of Health, Bethesda, Maryland 20892, United States

Gary A. Sulikowski,
Department of Chemistry, Vanderbilt University, Nashville, Tennessee 37235, United States; Vanderbilt Institute of Chemical Biology, Vanderbilt University, Nashville, Tennessee 37235, United States

Zhongyue J. Yang,
Department of Chemistry, Vanderbilt University, Nashville, Tennessee 37235, United States; Vanderbilt Institute of Chemical Biology, Vanderbilt University, Nashville, Tennessee 37235, United States

Giuseppe Bifulco,
Dipartimento di Farmacia, Università di Salerno, 84084 Fisciano (SA), Italy

Hyo-Moon Cho,
Laboratory of Bioorganic Chemistry, 8 Center Drive, National Institute of Diabetes and Digestive and Kidney Diseases, National Institutes of Health, Bethesda, Maryland 20892, United States

Christopher R. Fullenkamp
Department of Chemistry, Vanderbilt University, Nashville, Tennessee 37235, United States

CONSPECTUS:

Natural products have played an indispensable role in the discovery and development of antibiotics, antineoplastics, and therapeutics for other diseases. Natural products are unique among

[*]**Corresponding Author:** Carole A. Bewley – *Laboratory of Bioorganic Chemistry, 8 Center Drive, National Institute of Diabetes and Digestive and Kidney Diseases, National Institutes of Health, Bethesda, Maryland 20892, United States;* caroleb@mail.nih.gov.

Author Contributions

CRediT: All authors performed experiments and analyzed data. C.R.F. data curation (supporting), formal analysis (supporting). C.A.B. and G.A.S. wrote the first draft of the paper, and all authors contributed to the final version. CRediT: Christopher R Fullenkamp data curation (supporting), formal analysis (supporting).

ASSOCIATED CONTENT

Supporting Information

The Supporting Information is available free of charge at https://pubs.acs.org/doi/10.1021/acs.accounts.2c00648.

ECD, HRMS, and ^{1}H NMR spectra and coordinates for docked models (PDF)

Crystal structure of EcFtsZ (PDB)

Structure of chrysophaentin A compatible with STD-NMR (PDB)

Pose 1 of chrysophaentin A poorly compatible with STD-NMR (PDB)

Pose 1 of chrysophaentin A poorly compatible with STD-NMR (PDB)

DEDICATION

This Account is dedicated to the late Professor D. John Faulkner, on his 80th birthday, for his many contributions to the thriving field of marine natural products chemistry.

The authors declare no competing financial interest.

all other small molecules in that they are produced by dedicated enzymatic assembly lines that are the protein products of biosynthetic gene clusters. As the products of chiral macromolecules, natural products have distinct three-dimensional shapes and stereochemistry is often encoded in their structures through the presence of stereocenters, or in the case of molecules that lack a stereocenter, the presence of an axis or plane of chirality. In the latter forms of chirality, if the barrier to rotation about the chiral axis or chiral plane is sufficiently high, stable conformers may exist allowing for isolation of discrete conformers, also known as atropisomers. Importantly, the diverse functions and biological activities of natural products are contingent upon their structures, stereochemistry and molecular shape. With continued innovation in methods for natural products discovery, synthetic chemistry, and analytical and computational tools, new insights into atropisomerism in natural products and related scaffolds are being made. As molecular complexity increases, more than one form of stereoisomerism may exist in a single compound (for example, point chirality, chiral axes, and chiral planes), sometimes creating atypical or noncanonical atropisomers, a term used to distinguish physically noninterconvertable atropisomers from typical atropisomers.

Here we provide an account of the discovery and unusual structural and stereochemical features of the chrysophaentins, algal derived inhibitors of the bacterial cytoskeletal protein FtsZ and its associated protein partners. Eleven members of the chrysophaentin family have been discovered to date; seven of these are macrocyclic bis-bibenzyl ethers wherein the site of the ether linkage yields either a symmetrical or asymmetrical macrocyclic ring system. The asymmetrical ring system is highly strained and corresponds to the compounds having the most potent antimicrobial activity among the family. We review the structure elucidation and NMR properties that indicate restricted rotation between axes of two biaryl ethers, and the plane represented by the substituted 2-*Z*-butene bridge common to all of the macrocycles. Computational studies that corroborate high barriers to rotation about one representative plane, on the order of 20+ kcal/mol are presented. These barriers to rotation fix the conformation of the macrocycle into a bowl-like structure and suggest that an atropisomer should exist. Experimental evidence for atropisomerism is presented, consistent with computational predictions. These properties are discussed in the context of the total synthesis of 9-dechlorochrysophaenin A and its ring C isomers. Last, we discuss the implications for the presence of enantiomers in the biological activity and macrocyclization of the natural product.

Graphical Abstract

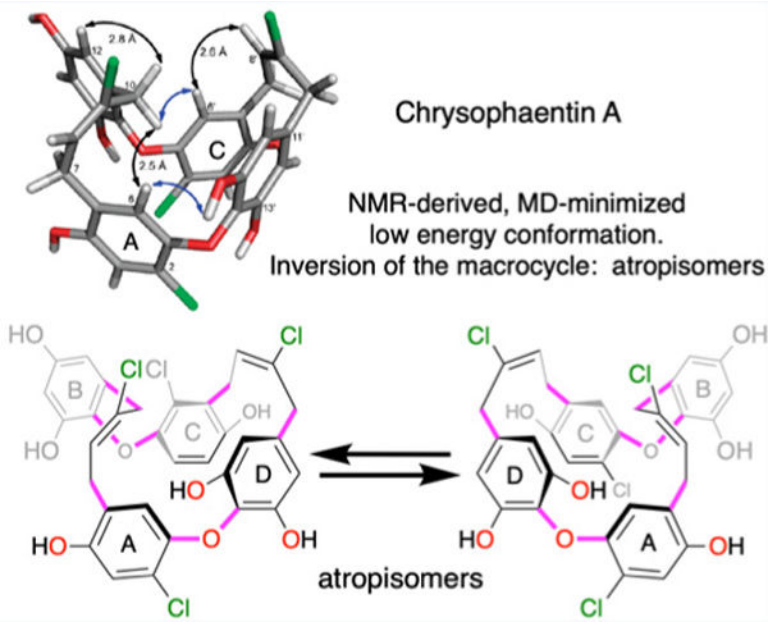

ATROPISOMERISM IN NATURAL PRODUCTS

Natural products, or DNA-encoded small molecules from Nature, comprise an enormous number of biologically active molecules whose chemical composition ranges from small organic compounds to complex, multicyclic peptides.[5] Accordingly natural products represent a wealth of chemical and structural diversity not found among synthetic compounds and generally not conceived of by chemists or biologists. Their unique architectures have long served as a source of inspiration and admiration to organic chemists, especially practitioners of total synthesis. As the biosynthetic products of complex, enzymatic assembly lines, most natural products are chiral. Their three-dimensional structures are intimately associated with stereochemistry, most frequently as a point of chirality due to carbon's ability to serve as a tetrahedral stereocenter (cf. (*R*) or (*S*) configuration) or chiral center. Less frequent forms of chirality in natural product architecture result from atropisomerism [of Greek origin, a (not) and tropos (turn)] (Figure 1). Among natural products, the most common group of atropisomers are polyketide-derived biaryls. Examples include the fungal metabolites viriditoxin,[6] a C_2 symmetrical naphtho-α-pyrone, and rugulotrosin A,[7] a C_2 symmetrical xanthone. In contrast to tetrahedral carbons that possess point chirality, biaryls with hindered rotation display axial chirality resulting in resolvable stereoisomers. In viriditoxin and rugulotrosin A, substitution around the biaryl carbon–carbon bond hinders rotation about the chiral axis and single enantiomers exist at room temperature (Figure 1A). Typically, for atropisomers to be separable at room temperature the energy barrier to rotation must be at least 23–25 kcal/mol, corresponding to a half-life of ≥1000 s.[8] Absolute configurations can be assigned by viewing down the chiral axis and prioritizing substituents at positions ortho to the central carbon–carbon bond.[9]

A third type of chirality observed in nature is planar chirality where a plane is defined by a group of atoms. *trans*-Cyclooctene is one of the simplest examples of a macrocycle with

planar chirality. Here the plane comprises the central alkene, associated trans hydrogens, and allylic carbons (Figure 2B). For racemization to occur, the remaining four carbons must move away from the plane with a twisting motion. That rotational barrier of 35 kcal/mol is sufficiently high to separate atropisomers at room temperature.[10] Numerous natural products and natural cyclophanes contain chiral planes and restricted rotation within the scaffold leads to atropisomers and/or enantiomers. This is illustrated in the pair of diaryl ether heptanoids acerogenin and (+)-galeon (Figure 1B). In the latter, the methoxy substituent positioned ortho to the ether oxygen atom gives configurationally stable atropisomers, with a calculated barrier to rotation of 45 kcal/mol compared to the nonsubstituted analog acrogenin, with an 8.8 kcal/mol barrier.[11]

With increasing complexity, certain natural products contain both axial and planar chirality, or even multiple elements of each. The glycopeptide antibiotic vancomycin provides a classic example.[12] This heptapeptide is the product of a seven-module nonribosomal peptide synthetase; three cytochrome P450s install biaryl and biaryl-ether cross-links to create its rigid three-dimensional structure (Figure 1C). Hindered rotation about the biaryl axis connecting rings A-B and the ether bonds connecting rings C–D and D-E stabilize the glycopeptide in the atropisomeric form shown. The biosynthesis of vancomycin is stereospecific and the isomer shown in Figure 1C is the only atropisomer observed in the *Amycolatopsis* producers.[12,13]

Most recently, an underappreciated example of atropisomerism was described by the Baran and Clardy groups for the natural product tryptorubin, a rigid bicyclic ribosomal peptide. When a total synthesis of the non-natural form of tryptorubin showed NMR data distinct from those of the natural material,[14,15] an atrop-specific total synthesis of the natural form revealed atropisomerism attributed to the position of the bridging macrocycle. Illustrated in Figure 1D, atropisomerism at the stage of the seco acid intermediate determines the position of the bridging macrocycle, above or below the plane of the macrocyle shown. The size and configuration of the bismacrocyclic product results in a physically noninterconvertable atropisomer that the authors refer to as noncanonical. Other strained macrocyclic atropisomers are represented in both natural products and synthetic molecules. Although a chiral axis or stereocenter may be absent in such macrocycles, restricted inversion of a ring gives rise to conformational chirality.[16] Examples include haouamine A[17,18] and (7'*S*, anti)-streptorubin B,[19] and a series of [para]cyclophanes (13, 14, and 15-membered macrocycles) chemoenzymatically synthesized by lipase-catalyzed acylations of a benzylic diol.[20] Similarly, the alga-derived, antimicrobial and macrocyclic natural product chrysophaentin A and some family members (chrysophaentins F–H) contain multiple stereochemical elements common to atropisomers;[1] in particular, although this family does not contain a stereocenter, chrysophaentin A contains several novel elements of chirality owing to its complex structure and restricted rotation in more than one plane. As part of this issue highlighting the synthesis, analysis and applications of atropisomers, we discuss the atropisomeric properties of chrysophaentin A, their implications for total synthesis, macrocyclization, and biological function.[2,4,21]

CHRYSOPHAENTINS: DISCOVERY, STRUCTURE, AND MECHANISTIC STUDIES

The antimicrobial chrysophaentins were originally discovered from a methanolic extract of *Chrysophaeum taylorii* by Lewis and Bryan (Pelagophyceae), a rare microalga observed on Mediterranean, Caribbean, and Australian coasts.[22,23] Structurally the chrysophaentins define a new class of marine natural products, namely, the bis-diarylbutenes (Figure 2A). While they resemble bis-bibenzyl natural products, mainly associated with liverworts,[24] the extension by two carbon atoms and presence of a “cis” 2-butene linker is unique to the chrysophaentins and in part engenders the molecules with conformational restrictions thus far exclusive to this alga. The bis-diarylbutene moieties in each half of the chrysophaentins include a 1,4-dihydroxy-2-Cl-phenyl ring and a 1,3-dihydroxy-substituted phenyl ring connected by the 2-butene linker. Differences in halogenation (Cl versus Br) and the site of macrocyclization between rings B and C lead to the diversity among chrysophaentin family members. Notably the ether bond connecting the A and D rings is invariable among all analogs while the B and C rings are connected ortho to the 2-butene linkage in chrysophaentins A–D (C-16 in Figure 2A, red), and para to the 2-butene in chrysophaentins F–H (C-14 in Figure 2A, blue). Chrysophaentins E–E3 are linear analogs and presumed precursors to the mature natural product.[3]

An estimated global minimum conformation of chrysophaentin A was obtained earlier by NMR analysis (select rotating frame NOEs, or ROEs are indicated) followed by molecular dynamics and PRCG (Polak–Ribier Conjugate Gradient) minimization (Figure 2B).[1] The minimum energy structure shown in Figure 2 reveals three chiral planes residing along rings A, B and C. Rotation about the highlighted bonds would result in interconversion to the corresponding enantiomer (Figure 2C). As represented, a high enough energy barrier would dictate an atropoenantiomeric relationship (see below).

Chrysophaentin A was the major product isolated from the original collection made in the southern side of St. John Island, USVI, and is the most active against *Staphylococcus aureus* (SA), methicillin-resistant SA (MRSA), and multidrug resistant SA (MDR-SA) with MICs around 2–4 μg/mL, followed by chrysophaentins F and H that are 2–5 times less potent.[1,21] The least potent or inactive chrysophaentins (D, G, and H) have Br substituents on the A and/or C arenes. Taken together the antimicrobial assays indicate that the ortho connectivity between rings B and C, and the presence of Cl substituents at C-2 and C-2’ on rings A and C are critical for activity, with potency decreasing in the corresponding brominated analogs (chrysophaentins B–D and G). Antimicrobial activity of the linear intermediate chrysophaentin E was reduced by ca. 5 to >12-fold toward the panel of strains tested.

SYNTHESIS OF 9-DECHLORO-CHRYSOPHAENTIN A, NMR EVIDENCE FOR HINDERED ROTATION

Studies of the antimicrobial activity, mechanism of action and structural properties of chrysophaentin A had been hampered due to the variable and limited availability of its natural producer. As an alternative, laboratory cultures of the producing alga were

examined as a source of chrysophaentin A but proved unsuccessful, with bis-bibenzyls as opposed to diaryl ethers and putative shunt products produced in culture.[3] As a source of natural products total synthesis remains advantageous relative to other approaches, as synthesis often provides access to structural analogs in support of mechanistic studies as well as efforts directed toward therapeutic development. In 2020 we described the total synthesis and antimicrobial activity of 9-dechlorochrysophaentin A and several congeners.[4] Selection of 9-dechlorochrysophaentin A as the primary synthetic target emerged from tactical and strategic considerations during the synthesis (Figure 3A). As a bis-aryl ether incorporating two trisubstituted cis alkene spacers, chrysophaentin A presents a significant synthetic challenge.[21,25,26] Specifically, the site of ring closure is not obvious. While ring-closing metathesis has enabled access to a variety of macrocycles incorporating alkenes of various geometry and substitution patterns, halogenated alkenes remain problematic. For this reason, we elected to simplify the chrysophaentin A problem to a macrocyclic cis alkene or 9-dechlorochyrophaentin A (Figure 3A). A second tactical decision was to initially merge the BC and AD bis-aryl ethers by an O-alkylation leading to an allylic ether that would subsequently be subjected to a Lewis acid promoted O to C migration. The latter conveniently proved to be unselective, with the migration nearly equally distributed between carbons C3′ and C5′. Ether bond formation at C5′ ultimately led to iso-9-dechlorochrysophaentin, and this analog has yielded insight into the effects of C ring substitution on atropisomeric properties compared to the natural C ring substitution (Figure 3A). An overview of our synthetic route leading to 9-dechlorochyrophaentin A and iso-9-dechlorochrysophaentin A is shown in Figure 3C. Highlights of the synthesis include coupling of AD and BC fragments by way of a Mitsunobu reaction followed by a Z-selective ring closing metathesis (RCM) reaction employing Grubbs' C633 catalyst.[27] Lewis acid ($BF_3{\cdot}OEt_2$) promoted O to C migration afforded a mixture of isomeric products that were separated following removal of isopropyl protecting groups. In addition to providing access to iso- and 9-dechlorochrysophaentins, two D ring dimethyl ether derivatives were prepared (VU0848355 and VU0848354, Figure 3B) that have proven useful in studies on conformational properties of this group of bis-aryl ether macrocycles.

Comparison of ^{1}H NMR spectra of methyl ethers VU0848355 and VU0848354 revealed that in VU0848355, signals corresponding to aromatic hydrogens H12' and H16' of the D ring are not observed at rt (+23 °C), but in variable temperature NMR experiments appear at lower temperatures (−20 to −40 °C, Figure 4A). This indicates that the rate of rotation at rt is similar to the NMR time scale, and rotation may be slowed at lower temperatures rendering the signals observable. When a similar variable temperature experiment was conducted on VU0848354 the singlet corresponding to H12' and H16' (Figure 4B), now homotopic, reached coalescence at lower temperature (−20 to −40 °C).[28] These experiments imply VU0848355, that has the natural chrysophaentin A C-ring substitution, possesses a higher rotational barrier for the observed atropisomeric NMR behavior relative to iso-chrysophaentin (VU0848354) where coalescence is observed at lower temperature.

ATROPISOMERISM IN CHRYSOPHAENTIN A

Three-Dimensional Conformation Reveals Inherent Chirality Attributed to Its Curvature

Among the eight chrysophaentin analogs and three hemichyrsophaentin analogs isolated to date, chrysophaentin A remains the major metabolite and most potent antimicrobial among the panel.[1,3] For that reason, earlier structural and functional studies were performed on chrysophaentin A. In a previous study global minimum energy calculations were performed to give a low energy conformer of chrysophaentin A that proved necessary to confirm the macrocyclic structure assigned by NMR, and to be used for molecular docking studies. Those calculations revealed a three-dimensional, bowl-like structure whose conformation appears to be locked in place by the presence of the biaryl ether moieties, and importantly, the 2-*Z*-butene linkers (Figure 2B). Interestingly, the bowl-like structure depicted in Figure 2C showed inherent chirality, as its intrinsic curvature makes it nonsuperimposable on its mirror image. In molecular dynamics simulations racemization (Figure 2C) of chrysophaentin A through inversion of its curvature was never observed.

To establish whether chrysophaentin A might exist as an atropisomer as indicated by MD simulations, an ECD spectrum of **1** was obtained and showed a strong positive Cotton effect at 207 and a weaker peak at 213 nm (Figure 5A). A theoretical ECD curve is similar to the experimental with strong positive Cotton effects predicted at 206 and 216 nm. To investigate whether atrop-**1** (i.e. **2**, red) or a racemic mixture of putative atropenantiomers exists, we used RP-HPLC-MS to analyze separate chromatographic fractions previously generated from Sephadex LH20 chromatography of extracts of *C. taylorii*. (None of those fractions exhibited anti-*Staphylococcal* activity.) Three fractions eluting with the same retention time and showing identical molecular ions by LRMS and HRMS (Figures 5B–D, S1, and S2) were identified with one containing ca. 300 μg of material (referred to as **2**, or atrop-**1**). NMR spectra of **2** were identical to those of the originally isolated chrysophaentin A (Figures 5E and S3). However, the ECD spectra for these separate fractions showed very small to zero positive Cotton effects indicated partial racemic mixtures (Figure S1). Thus, while the chromatographic behavior and spectral data of **2** are identical to those of **1**, the greatly reduced magnitude of the observed Cotton effect indicates the presence of a mixture of atropenantiomers.

A re-evaluation of the binding mode of chrysophaentin A with a recently solved high resolution crystal structure of *Escherichia coli* FtsZ (EcFtsZ) released in 2020 (PDB code: 6UNX) confirmed the observations that the chrysophaentin A stereoisomer published in 2010 shows binding poses compatible with the STD-NMR data (Figure 5). On the contrary, crucial interactions for H-3 and H-3′ are missing in the docking poses for the enantiomeric species (Figure S4). A visual inspection of the energetically most favorable binding poses of chrysophaentin A to EcFtsZ shows the natural product to be surrounded by residues in the GTP binding site, consistent with the ability of chrysophaentin A to displace GTP in a competitive manner (Figure 6).[1] In contrast, the binding poses for the enantiomeric species of chrysophaentin A show the ligand to be mostly extruded from the protein (Figure S4) and nonoverlapping with GDP (the ligand captured in the crystal structures).

Computational Support for Restricted Bond Rotation in Chrysophaentins

Chrysophaentin A contains three hypothetical chiral planes located along the two 2-*Z*-butene linkers connecting rings A and B, and C and D, and the ring B/C interface. In extended molecular dynamics simulations, interconversion between the two atropisomers was never observed, suggesting a high kinetic barrier to racemization. The conversion between the two enantiomers is expected to involve changes in all dihedral angles associated with chiral planes, and multiple steps of ring flipping. To investigate one such elementary step for conversion between enantiomeric atropisomers, we computed the energetics for ring flipping between ring B and ring C using a two-dimensional energy scan (Figure 7A). (Rings B and C were chosen on account of the variable temperature NMR experiments where the barrier to rotation of ring D appears to be affected by the connectivity and orientation of ring C.) The coordinates selected in the energy scan include those for two dihedral angles. Dihedral 1 is defined by C16–O–C1′–C2’ connecting rings B and C; and dihedral 2 defined by C5′–C7′–C8′–C9’ consists of the eastern 2-Z-butene linker forming the plane that connects rings C and D (Figure 7B). Notably, the flipping motion leads to a transient diastereomeric conformational state (Figure 7B). Considering all possible combinations between the two dihedral angles gives 360 structures. For the sake of computational cost, all structures were computed using a semiempirical QM method (PM6) with dihedral 1 and dihedral 2 constrained during optimization.

The energy scan calculation shows that rotating dihedral 1 alone is not sufficient for the atropoisomeric flipping between rings B and C. The flipping only occurs within a limited range for dihedral 2 (between 74 and 174 degrees). This suggests that cooperative motion between these two dihedral angles is necessary for inversion of rings B and C. Based on the 2D energy scan, we identified the lowest energy path and conducted higher-level QM optimization for estimation of the flipping barrier (i.e., B3LYP/6–31G(d,p) method with dihedrals 1 and 2 constrained). The hypothetical transition structure was identified (Figure 6C) with a barrier of 11.6 kcal/mol. Although the computed barrier is only a fraction of the total energetic cost for atropisomeric racemization, this represents one step toward inversion of the chrysophaentin macrocycle and suggests that concerted bond rotations about all stereochemical elements will be required for inversion of atropisomers.[30] To investigate the entire molecular process for enantiomeric conversion, it will be necessary to compute the energetics of the motions with respect to rings A and B and rings C and D. In addition, the possibility of synergistic multiring flipping should be assessed. This can be potentially accomplished using molecular dynamics simulations with enhanced sampling.[31,32]

RELEVANCE TO BIOLOGICAL ACTIVITY AND TARGET ENGAGEMENT

Chrysophaentin A (the major compound in the original collection from the southern side of St. John Island, USVI) was the most active family member in inhibiting the growth of *Staphylococcus aureus* (SA), methicillin-resistant SA (MRSA), and multidrug resistant SA (MDR-SA), followed by chrysophaentins F and H. In vitro experiments using the recombinant cytoskeletal proteins EcFtsZ and *S. aureus* FtsZ (SaFtsZ) revealed that chrysophaentin A inhibits the GTPase activity of both species of FtsZ in GTPase enzyme assays and prevents assembly of FtsZ into protofilaments, a critical step for cell

division. NMR competition experiments with chrysophaentin A and recombinant EcFtsZ protein revealed that the natural product can competitively displace GTP from FtsZ, and saturation transfer difference (STD) NMR spectra allowed mapping of the protons that are in close proximity to FtsZ when the ligand is bound. Molecular docking of the two atropisomers strongly suggests that only one form (Figure 2B) can contact FtsZ in a pose that is consistent with the STD NMR data and would allow for displacement of GTP by chrysophaentin A. In vivo experiments using live bacteria later corroborated this activity. First, confocal microscopy employing the fluorescent protein fusion constructs YFP-EcFtsZ and mCherry-EcFtsZ in an Env-permeable *E. coli* strain showed that treatment of bacterial cells with chrysophaentin A inhibited Z-ring and bacterial septum formation, indicating inhibition of FtsZ assembly by the natural product.[2] More recently, chrysophaentin A and 9-dechlorochrysophaentin A were shown by fluorescence microscopy to completely delocalize FtsZ, to dissociate its partner proteins FtsZ and PBP2B (penicillin binding protein 2B) from the division plane, and to inhibit the uptake of fluorescently labeled amino acids in *Bacillus subtilis*, indicating inhibition of cell wall biosynthesis.[4] In antimicrobial assays and in vitro biophysical studies, the natural enantiomeric form of chrysophaentin A (**1**) is more potent than natural or synthetic analogs or chrysophaentin fragments. MD simulations also indicate a preference for enantiomer **1** binding to the target FtsZ. However, microscopy studies indicate that 9-dechlorochrysophaentin and its isomer also inhibit Z-ring assembly and function. The concentrations of synthetic products used for microscopy studies slightly exceed the MIC concentrations making it impossible to distinguish differential binding between **1** and its nonatropisomeric analogs. Future studies will be necessary to experimentally demonstrate a preference, and that must include investigations of newly collected algae for the existence of the atropoenantiomer.

CONCLUSIONS

The study of atropisomerism in natural products and synthetic scaffolds continues to be a fruitful area of research and is critical to understanding the effects of atropisomers on their chemical and biological functions.[33,34] Features that make the chrysophaentin A scaffold in particular unique from other atropisomeric natural products include the 2-chloro-2-*E*-butene linker that connects two asymmetrically linked diaryl ethers. Interestingly, the “trans” isomer, namely, 2-chloro-2-*Z*-butene, has never been observed in NMR spectra of any chrysophaentin, whether originating from field collections or laboratory culture of the producing alga *C. taylorii*. The chrysophaentins bear a close resemblance to the marchantin family of natural products, except that the marchantins typically contain an ethano rather than a butene bridge.[24] A notable exception is cavicularin, an optically active cyclic bibenzyl-dihyrophenanthrene wherein coupling of one of the ethano-linked benzyl moieties creates a strained and rigid macrocycle (Figure 8). Evidence for planar chirality and atropisomerism among the bis-bibenzyls and macrocyclic natural products in general, has come from total syntheses, exemplified by cavicularin,[35,36] abyssomycin,[37] and haouamine A to name a few (Figure 8); and computational studies, chiral separations, and NMR. Pattawong et al. used quantum mechanical calculations to develop predictive rules for racemization barriers in diaryl ether heptanoid (DAEHs) natural products that encompass multiple and concerted dihedral bond rotations. Relevant to the chrysophaentins,

those studies indicate that stereoisomerization requires torsional rotations of all stereogenic elements, and introduction of an olefin into the ansa bridge dramatically increased the barrier to rotation.[30] Currently, it is not possible to predict the barriers to rotation for macrocylces as complex as the members of the marchantin family, the chrysophaentins, and other configurationally stable atropisomers such as abyssomycin and acerogenin.[11] Experimental data connecting optical activity and, for example, X-ray crystallography or Cotton effects in ECD spectra are lacking. These are areas ripe for discovery and are important to understanding and predicting atropisomerism.

Supplementary Material

Refer to Web version on PubMed Central for supplementary material.

ACKNOWLEDGMENTS

We thank J. L. Keffer for chromatographic separations, R. D. O'Connor and D. Stec for assistance with NMR spectra, J. Lloyd for HRMS data, and the Vanderbilt Institute for Chemical Biology and the NIH Intramural Research Program (NIDDK) for funding.

Biographies

Carole A. Bewley received her Ph.D. from Scripps Institution of Oceanography, University of California, San Diego with the late Professor. D. John Faulkner working in marine natural products chemistry. She was a Cancer Research Institute Postdoctoral Fellow in the Laboratory of Chemical Physics, NIDDK, NIH, working in structural biology using macromolecular NMR. She started her independent career as a tenure track investigator in the Laboratory of Bioorganic Chemistry, NIDDK, at the National Institutes of Health. She is currently a Senior Investigator and Chief of the Laboratory of Bioorganic Chemistry, and the Natural Products Chemistry Section.

Gary A. Sulikowski received a B.S. in chemistry from Wayne State University and a Ph.D. in organic chemistry from the University of Pennsylvania with Professor Amos B. Smith, III. He was an American Cancer Society postdoctoral fellow at Yale University with Professor Samuel Danishefsky. His first faculty appointment was in the Department of Chemistry at Texas A&M University in 1991 and joined the Vanderbilt Chemistry Department and Institute of Chemical Biology in 2004. He assumed the role of the Director of the Vanderbilt Institute of Chemical Biology in 2017. He is the Faculty Director of the Institute of Chemical Biology Chemical Synthesis core, Stevenson Professor of Chemistry and Professor of Pharmacology.

Zhongyue (John) Yang is an Assistant Professor of Chemistry at Vanderbilt University. He received his B.S. in Chemistry in 2013 from the Po-Ling program at Nankai University and his Ph.D. in 2017 with Professor Kendall N. Houk at UCLA. From 2018–2020, he worked with Professor Heather Kulik as a postdoctoral scholar in the Department of Chemical Engineering at MIT. He started his independent career at Vanderbilt in 2020. He is a faculty member in the Department of Chemistry, Center for Structural Biology, Vanderbilt Institute of Chemical Biology, and Data Science Institute.

Giuseppe Bifulco graduated at University of Naples (Italy) with Prof. Luigi Minale and received a PhD in Organic Chemistry from the University of Naples with Professor Raffaele Riccio. He was a visiting scientist at the Scripps Research institute of La Jolla, CA, working on calcium-binding proteins with Prof. Walter Chazin and later working on the interactions between synthetic dimers of calicheamicin and DNA with Prof. K.C. Nicolaou. He is currently Professor of Organic Chemistry at the Department of Pharmacy of the University of Salerno where he is involved in the design, synthesis and studies of the mechanism of action of bioactive molecules with antitumor and anti-inflammatory activity, and in the development of new methodologies in the structural analysis of natural products using quantum mechanical calculations and advanced nuclear magnetic resonance techniques.

Hyo-Moon Cho received her PhD in Pharmacognosy from Seoul National University in 2020. Her research interests include natural products chemistry and the discovery of new biologically active metabolites using mass spectrometry and other spectroscopic methods for reliable and rapid compound identification. Dr. Cho has received lecture, research and academic scholarships from Seoul National University and the Korea Society of Pharmacognosy.

C**hristopher R. Fullenkamp** received his PhD in Chemistry from Vanderbilt University in 2020 working with Gary Sulikowski on the total synthesis of the antimicrobial natural product, chrysophaentin A. He is currently a CRTA postdoctoral fellow at the National Cancer Institute in the Chemical Biology Laboratory, developing nucleic acid interacting small molecules as novel therapeutics for cancer.

REFERENCES

(1). Plaza A; Keffer JL; Bifulco G; Lloyd JR; Bewley CA Chrysophaentins A-H, antibacterial bisdiarylbutene macrocycles that inhibit the bacterial cell division protein FtsZ. J. Am. Chem. Soc 2010, 132, 9069–9077. [PubMed: 20536175] This work describes the original discovery and structural characterization of the chrysophaentins and their targeting of the bacterial cytoskeletal protein FtsZ using NMR and biochemical assays.

(2). Keffer JL; Huecas S; Hammill JT; Wipf P; Andreu JM; Bewley CA Chrysophaentins are competitive inhibitors of FtsZ and inhibit Z-ring formation in live bacteria. Biorg. Med. Chem 2013, 21, 5673–5678.Using f luorescently labeled FtsZ constructs this work shows inhibition of Z-ring formation in live bacteria by the chrysophaentins.

(3). Davison JR; Bewley CA Antimicrobial Chrysophaentin Analogs Identified from Laboratory Cultures of the Marine Microalga *Chrysophaeum taylorii*. J. Nat. Prod 2019, 82, 148–153. [PubMed: 30623657] Laboratory cultures of Chrysophaeum taylorii, the chrysophaentin-producing alga, led to the isolation of new hemichrysophaentins and putative biosynthetic shunt products, to shed light on a proposed biosynthesis.

(4). Fullenkamp CR; Hsu YP; Quardokus EM; Zhao G; Bewley CA; VanNieuwenhze M; Sulikowski GA Synthesis of 9-Dechlorochrysophaentin A Enables Studies Revealing Bacterial Cell Wall Biosynthesis Inhibition Phenotype in *B. subtilis*. J. Am. Chem. Soc 2020, 142, 16161–16166. [PubMed: 32866011] Synthesis of iso- and 9-dechlorochrysophaentin A enabled by a Z-selective ring-closing metathesis macrocyclization followed by an oxygen to carbon ring contraction facilitated fluorescent microscopy studies showing inhibition of bacterial cell wall biosynthesis by disassembly of key divisome proteins.

(5). Pye CR; Bertin MJ; Lokey RS; Gerwick WH; Linington RG Retrospective analysis of natural products provides insights for future discovery trends. Proc. Natl. Acad. Sci. U. S. A 2017, 114, 5601–5606. [PubMed: 28461474]

(6). Suzuki K; Nozawa K; Nakajima S; Kawai K-I Structure revision of mycotoxin, viridotoxin, and its derivatives. Chem. Pharm. Bull. (Tokyo) 1990, 38, 3180–3181.

(7). Stewart M; Capon RJ; White JM; Lacey E; Tennant S; Gill JH; Shaddock MP Rugulotrosins A and B: Two new antibacterial metabolites from an Australian isolate of a Penicillium sp. J. Nat. Prod 2004, 67, 728–730. [PubMed: 15104517]

(8). Oki M Recent Advances in Atropisomerism. In Topics in Stereochemistry; Eliel EL, Alligner NL, Wilen SH, Eds.; Springer-Verlag: Berlin, 1983; Vol. 14, pp 1–81.

(9). Eliel EL; Wilen SH Stereochemistry of Organic Compounds; Wiley: New York, 1994.

(10). Schlögl K Planar Chiral Molecular Structures. In Stereochemistry; Vogtle F, Weber E, Eds.; Topics in Current Chemistry; Springer-Verlag: Berlin, 1984; pp 27–62.

(11). Salih MQ; Beaudry CM Chirality in diarylether heptanoids: synthesis of myricatomentogenin, jugcathanin, and congeners. Org. Lett 2012, 14, 4026–4029. [PubMed: 22804345]

(12). Barna JC; Williams DH The structure and mode of action of glycopeptide antibiotics of the vancomycin group. Annu. Rev. Microbiol 1984, 38, 339–357. [PubMed: 6388496]

(13). Boger DL; Miyazaki S; Loiseleur O; Beresis RT; Castle SL; Wu JH; Jin Q Thermal Atropisomerism of Aglucovancomycin Derivatives: Preparation of (M,M,M)- and (P,M,M)-Aglucovancomycins. J. Am. Chem. Soc 1998, 120, 8920–8926.

(14). Wyche TP; Ruzzini AC; Schwab L; Currie CR; Clardy J Tryptorubin A: A Polycyclic Peptide from a Fungus-Derived Streptomycete. J. Am. Chem. Soc 2017, 139, 12899–12902. [PubMed: 28853867]

(15). Reisberg SH; Gao Y; Walker AS; Helfrich EJN; Clardy J; Baran PS Total synthesis reveals atypical atropisomerism in a small-molecule natural product, tryptorubin A. Science 2020, 367, 458–463. [PubMed: 31896661]

(16). Bao X; Rodriguez J; Bonne D Enantioselective Synthesis of Atropisomers with Multiple Stereogenic Axes. Angew. Chem., Int. Ed 2020, 59, 12623–12634.

(17). Garrido L; Zubia E; Ortega MJ; Salva J Haouamines A and B: a new class of alkaloids from the ascidian *Aplidium haouarianum*. J. Org. Chem 2003, 68, 293–299. [PubMed: 12530851]

(18). Baran PS; Burns NZ Total synthesis of (±)-haouamine A. J. Am. Chem. Soc 2006, 128, 3908–3909. [PubMed: 16551088]

(19). Haynes SW; Sydor PK; Corre C; Song L; Challis GL Stereochemical elucidation of streptorubin B. J. Am. Chem. Soc 2011, 133, 1793–1798. [PubMed: 21166415]

(20). Gagnon C; Godin E; Minozzi C; Sosoe J; Pochet C; Collins SK Biocatalytic synthesis of planar chiral macrocycles. Science 2020, 367, 917–921. [PubMed: 32079773]

(21). Keffer JL; Hammill JT; Lloyd JR; Plaza A; Wipf P; Bewley CA Geographic variability and anti-staphylococcal activity of the chrysophaentins and their synthetic fragments. Mar. Drugs 2012, 10, 1103–1125. [PubMed: 22822360]

(22). Caronni S; Calabretti C; Cavagna G; Ceccherelli G; Delaria MA; Macri G; Navone A; Panzalis P The invasive microalga *Chrysophaeum taylorii*: Interactive stressors regulate cell density and mucilage production. Mar. Environ. Res 2017, 129, 156–165. [PubMed: 28583693]

(23). Piazzi L; Atzori F; Cadoni N; Cinti MF; Frau F; Ceccherelli G Benthic mucilage blooms threaten coralligenous reefs. Mar. Environ. Res 2018, 140, 145–151. [PubMed: 29921450]

(24). Harrowven DC; Kostiuk SL Macrocylic bisbibenzyl natural products and their chemical synthesis. Nat. Prod Rep 2012, 29, 223–242. [PubMed: 22089169]

(25). Vendeville JB; Matters RF; Chen A; Light ME; Tizzard GJ; Chai CLL; Harrowven DC A synthetic approach to chrysophaentin F. Chem. Commun 2019, 55, 4837–4840.

(26). Brockway AJ; Grove CI; Mahoney ME; Shaw JT Synthesis of the diaryl ether cores common to chrysophaentins A, E and F. Tetrahedron Lett 2015, 56, 3396–3401. [PubMed: 26034333]

(27). Herbert MB; Grubbs RH Z-selective cross metathesis with ruthenium catalysts: synthetic applications and mechanistic implications. Angew. Chem., Int. Ed. Engl 2015, 54, 5018–5024. [PubMed: 25802009]

(28). Fullenkamp CR Total Synthesis of 9-dechlorochrysophaentin Reveals a Novel Mechanism of Cell Wall Biosynthesis Inhibition. Doctoral dissertation, Vanderbilt University, Nashville, TN, 2020.

(29). Schumacher MA; Ohashi T; Corbin L; Erickson HP High-resolution crystal structures of *Escherichia coli* FtsZ bound to GDP and GTP. Acta Crystallogr. F Struct. Biol. Commun 2020, 76, 94–102. [PubMed: 32039891]

(30). Pattawong O; Salih MQ; Rosson NT; Beaudry CM; Cheong PH The nature of persistent conformational chirality, racemization mechanisms, and predictions in diarylether heptanoid cyclophane natural products. Org. Biomol. Chem 2014, 12, 3303–3309. [PubMed: 24736446]

(31). Yang YI; Shao Q; Zhang J; Yang L; Gao YQ Enhanced sampling in molecular dynamics. J. Chem. Phys 2019, 151, 070902. [PubMed: 31438687]

(32). Petraglia R; Nicolaï A; Wodrich MD; Ceriotti M; Corminboeuf C Beyond static structures: Putting forth REMD as a tool to solve problems in computational organic chemistry. J. Comput. Chem 2016, 37, 83–92. [PubMed: 26228927]

(33). Smyth JE; Butler NM; Keller PA A twist of nature-the significance of atropisomers in biological systems. Nat. Prod. Rep 2015, 32, 1562–1583. [PubMed: 26282828]

(34). Scott KA; Ropek N; Melillo B; Schreiber SL; Cravatt BF; Vinogradova EV Stereochemical diversity as a source of discovery in chemical biology. CRCHBI 2022, 2, 100028.

(35). Zhao P; Beaudry CM Total synthesis of (±)-cavicularin: control of pyrone Diels-Alder regiochemistry using isomeric vinyl sulfones. Org. Lett 2013, 15, 402–405. [PubMed: 23301524]

(36). Zhao P; Beaudry CM Enantioselective and regioselective pyrone Diels-Alder reactions of vinyl sulfones: total synthesis of (+)-cavicularin. Angew. Chem., Int. Ed. Engl 2014, 53, 10500–10503. [PubMed: 25082270]

(37). Nicolaou KC; Harrison ST Total synthesis of abyssomicin C and atrop-abyssomicin C. Angew. Chem., Int. Ed 2006, 45, 3256–3260.

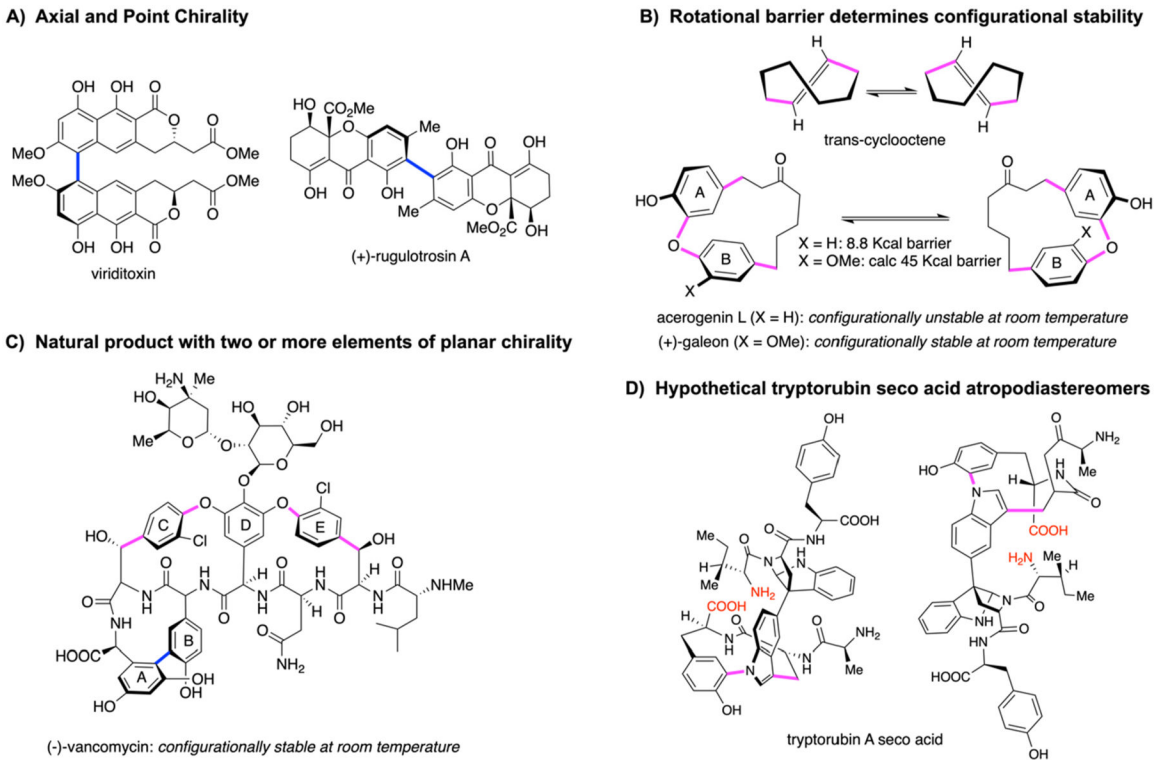

Figure 1.

Examples of atropisomerism in natural products. Blue and magenta bonds correspond to chiral axes and chiral planes, respectively.

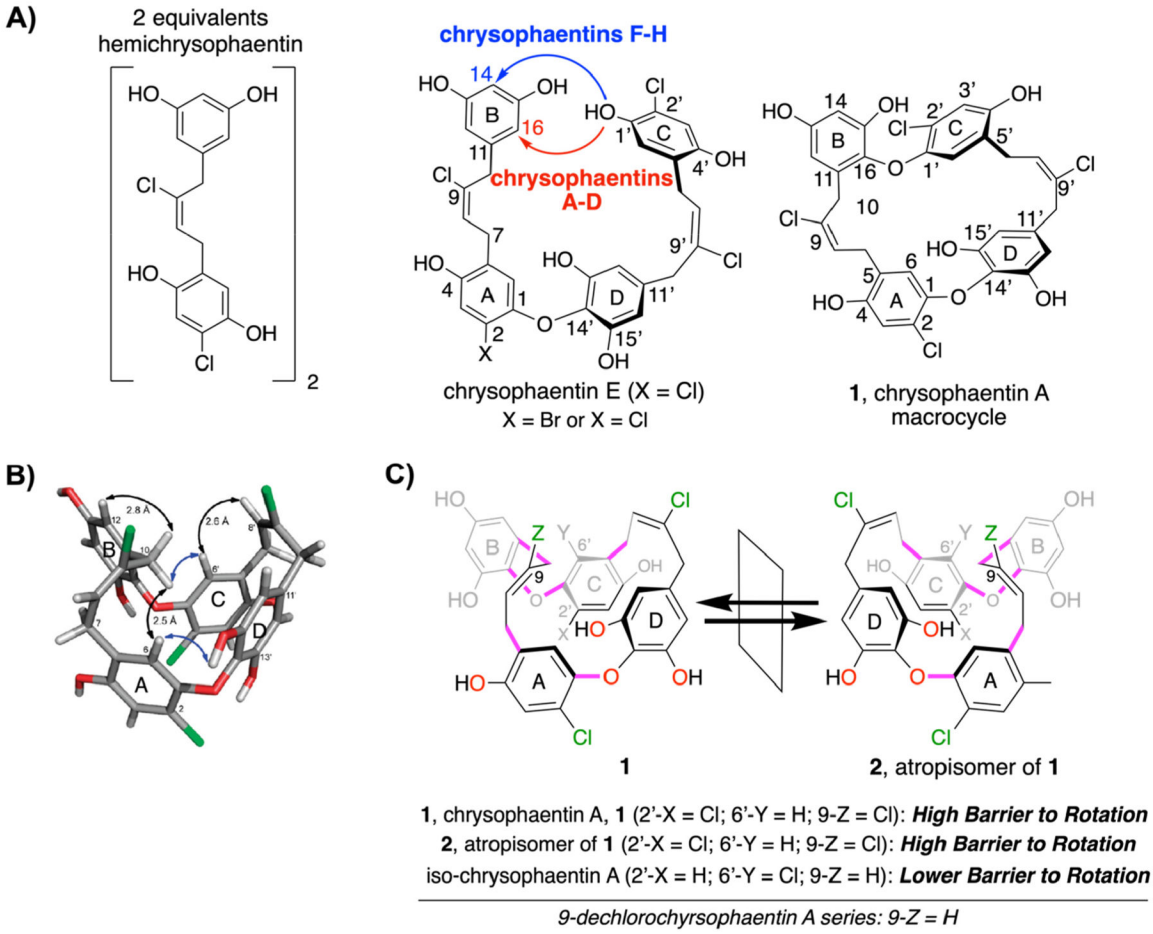

Figure 2.

Structural and conformational features of chrysophaentin A. (A) Hypothetical pathway leading to macrocycle formation through ether bond formation at C-16 (ortho substitution relative to C-11 2-butene linker) to give chrysophaentin A, or at C-14 (para substitution) to give chrysophaentins F–H (not shown).[1] (B) Lowest energy conformation of chrysophaentin A assigned by NMR analysis and energy minimization. (C) Interconversion of atropoenantiomers of chyrosophaentin A. Magenta bonds denote chiral planes.

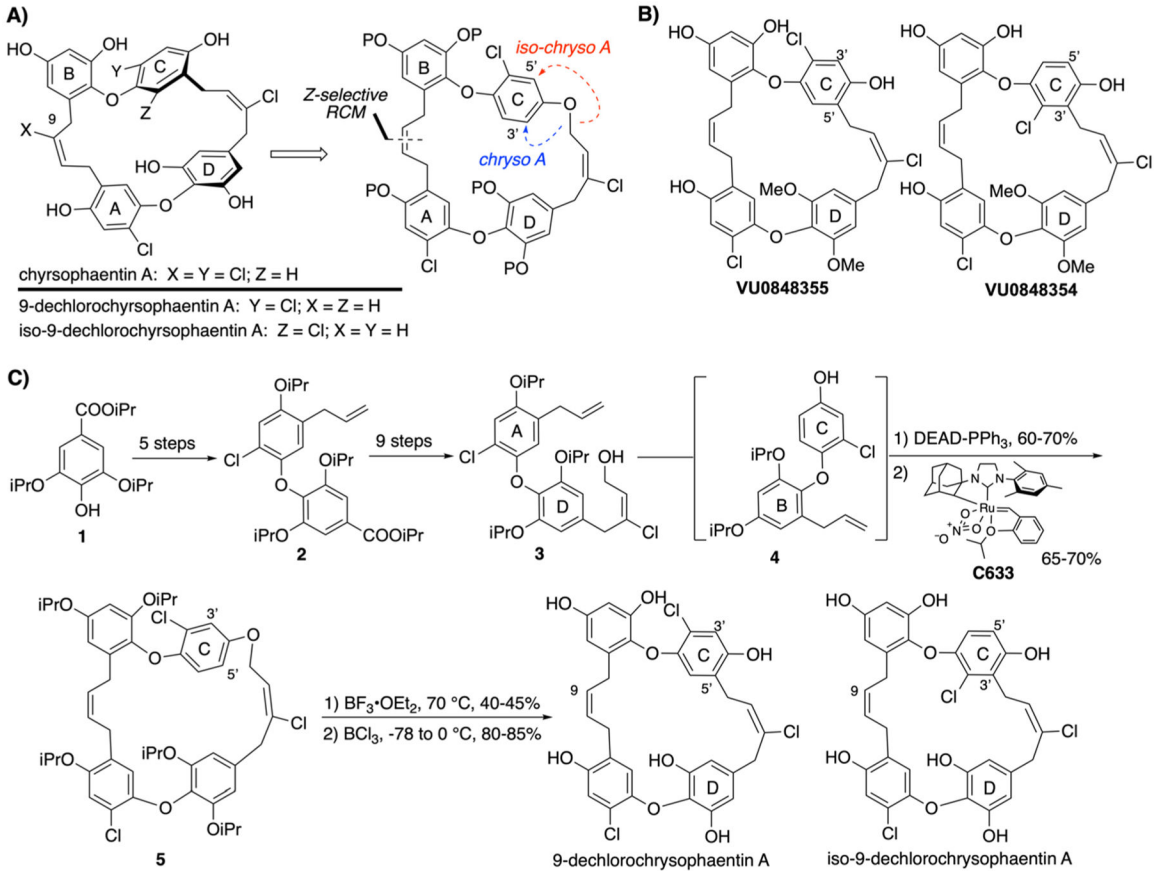

Figure 3.

Structures and synthetic scheme for 9-dechlorochrysophaentin A and iso-9-dechlorochrysophaentin A. (A) Comparison of chrysophaentin A and 9-dechlorochrysophaentin A as synthetic targets. (B) Structure of chrysophaentin congener methyl ethers VU0848355 (9-dechlorochrysophaentin) and VU0848354 (iso-9-dechlorochrysophaentin). (C) Abbreviated chemical synthesis of 9-dechlorochrysophaentin A and iso-9-dechlorochrysophaentin A.

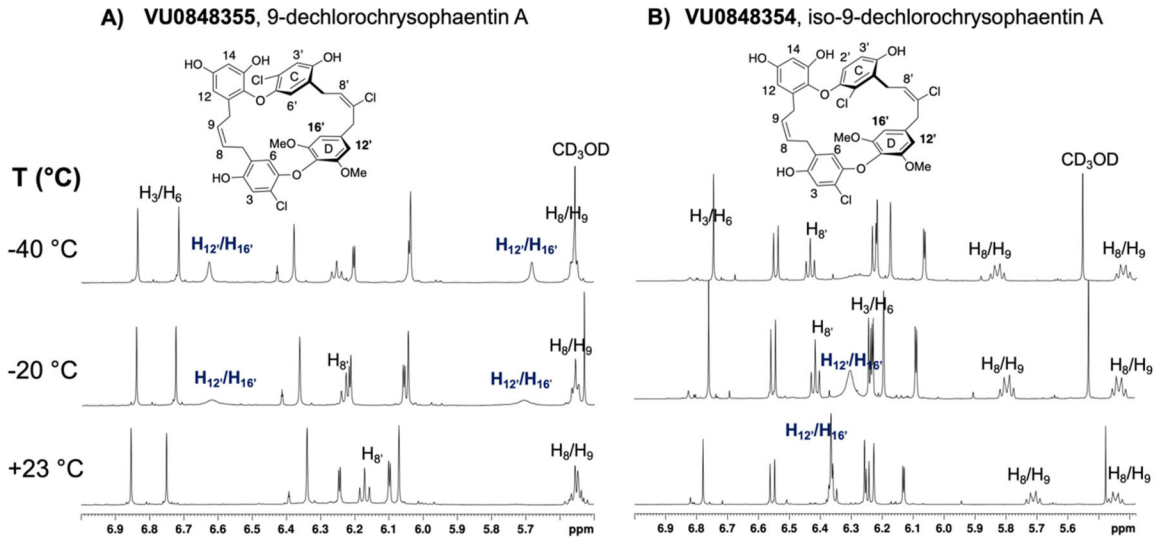

Figure 4.

Variable temperature ^{1}H NMR spectra for synthetic chrysophaentin analogs. (A) ^{1}H NMR spectrum of VU0848355, 9-dechlorochrysophaentin A; and (B) VU0848354, iso-9-dechlorochrysophaentin A. Spectra were acquired at 600 MHz in CD_3OD.

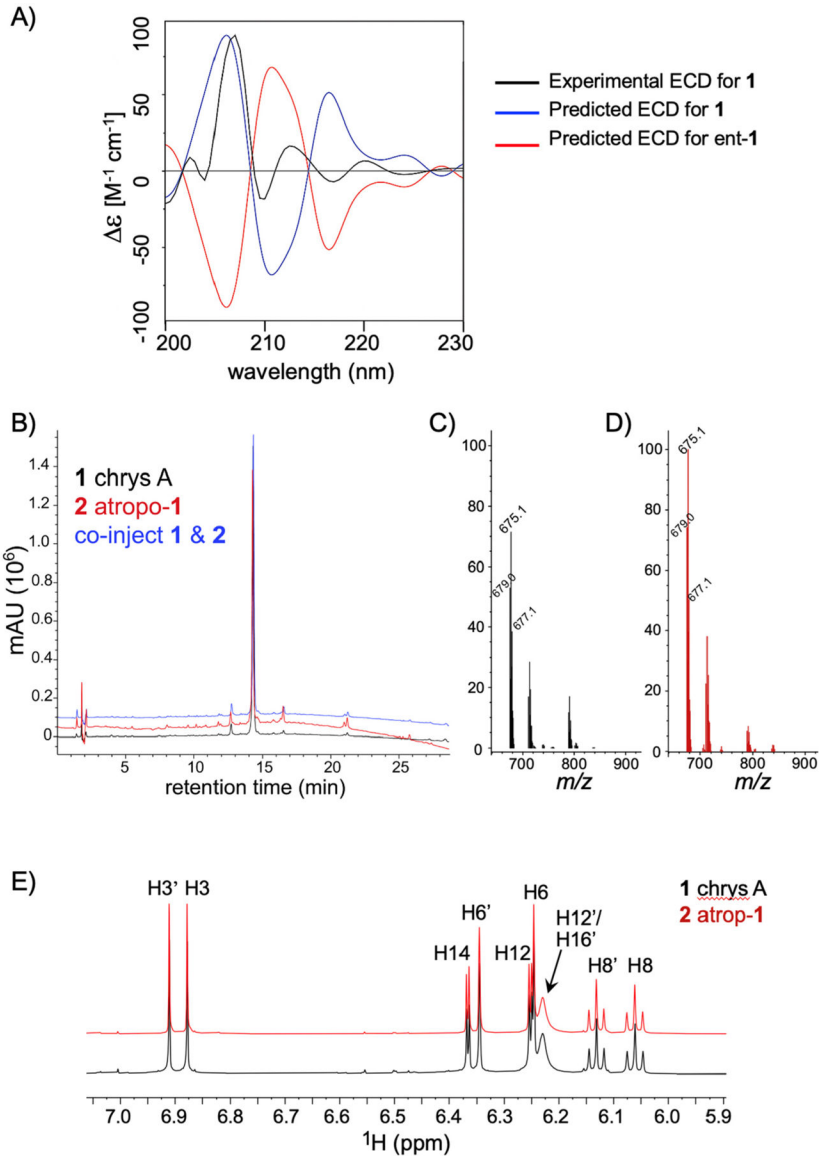

Figure 5.

Evidence for atropisomers in chrysophaentin A. Chromatographic and spectroscopic comparison of **1** (black) and an atropisomeric mixture of chrysophaentin A (**2**, red, referred to as atrop-chrysophaentin A) obtained from separate Sephadex LH20 chromatographic fractions of *C. taylorii*. (A) Experimental ECD spectrum of **1** (black) overlaid with the theoretical ECD spectra of **1** (blue) and its enantiomer (red). Experimental ECD spectra for **2** and additional fractions consisting of atropisomeric mixtures are shown in Figure S1. (B) Diode array and MS-detected chromatograms (254 nm and positive mode, respectively) of **1** (black), **2** (red) and coinjection of **1** and **2** (blue). (C,D) Mass spectra of the major peaks for **1** and **2** show identical molecular ions. The HRMS for **2** appears in Figure S2. (E) Downfield expansions from 5.9 to 7.2 ppm of the ^{1}H NMR spectra for **1** (black) and **2** (red). Aromatic and olefinic protons are labeled and spectra are superimposable; full spectrum appears in Figure S3.

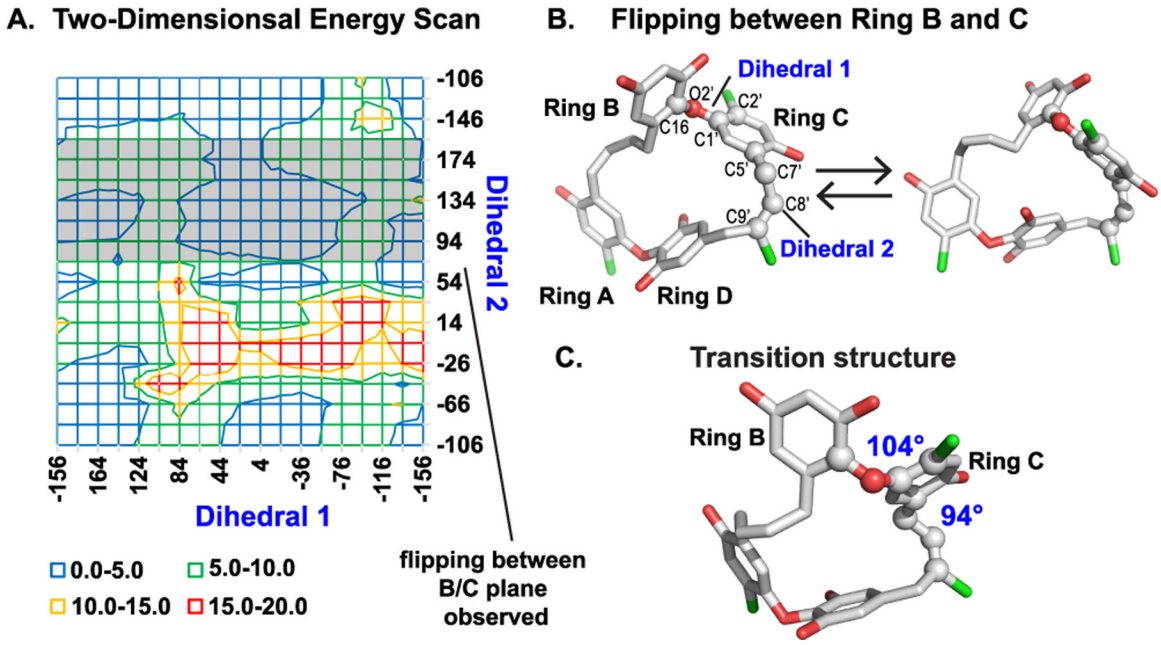

Figure 6.

Molecular docking pose of chrysophaentin A to *E. coli* FtsZ. The crystal structure of *E. coli* FtsZ, PDB code, 6UNX,[29] was used for docking. The low energy conformer of chrysophaentin A docks to the GTP binding site. Chrysophaentin A-EcFtsZ interactions are compatible with experimental Saturation Transfer Difference (STD) NMR data.

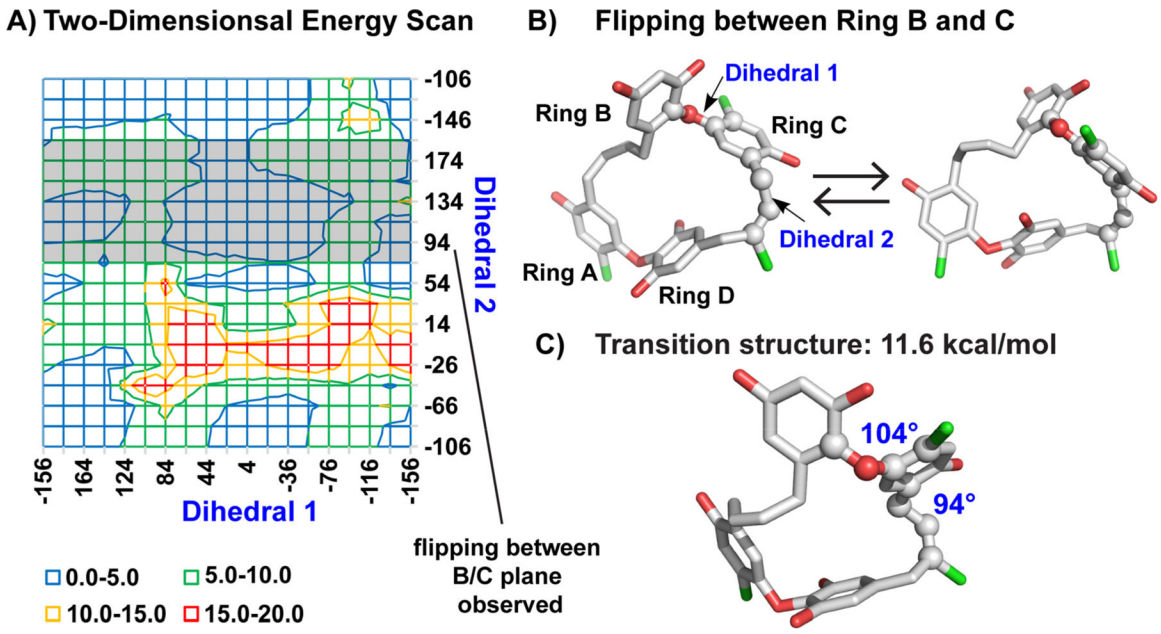

Figure 7.

Calculated energy for flipping of ring C as a step toward inversion of chrysophaentin A. (A) Two-dimensional energy scan for rotation about the planes connecting rings B/C and C/D. The starting geometries for the energy scan were obtained by conformational sampling of chrysophaentin A using the MMFF force field in Schrödinger, followed by DFT optimization using B3LYP/6–31G(d) in Gaussian16. Each dihedral angle was scanned over 360° with an interval of 20°. (B) Dihedrals 1 and 2 include atoms C16–O–C1′–C2’ and C5′–C7′–C8′–C9’ connecting rings B and C, and rings C and D, respectively. Atoms are shown as spheres. (C) A transition structure between flipping of rings B and C.

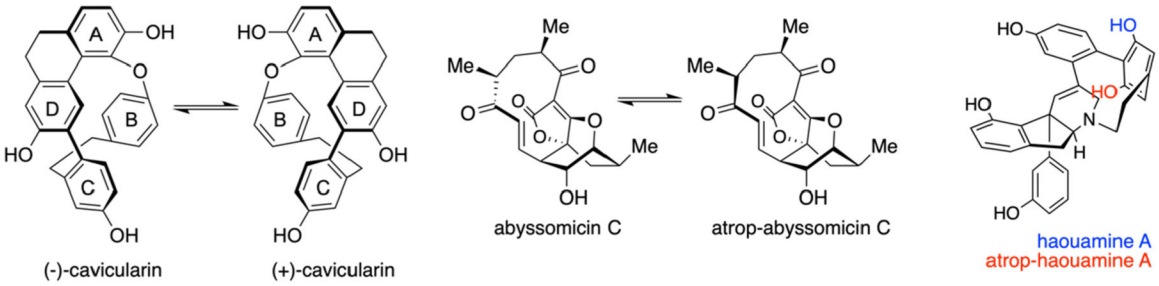

Figure 8.
Atropisomeric natural products with planar chirality proven by synthesis.